Chromism of spiropyrans

Kortekaas, Luuk

Chapter 6
Novel Reactivity in Bispiropyran Photochromes

Abstract Synthetic coupling of two spiropyrans was conducted through their photochrome, yielding a new class of spiropyran photochromes complete with novel reactivity. By direct tethering through their photoactive functional unit, cross-talk between the two components is achieved which affects their response in mainly the protonated state. Spiropyrans themselves we know to be capable of pH-gated photochromism, complete with thermal equilibration of the bidirectionally photoaccessible protonated *Z* and *E* isomer forms. These bispiropyrans, however, show complete thermal stability in the protonated *Z*- and *E*-isomer forms, while showing an unprecedented one-way reactivity to UV resulting in *Z* to *E* photoisomerization. Deprotonation of either protonated form swiftly resets the system to the bispiro ring-closed form through fast thermal relaxation. Furthermore, deprotonation of the protonated E form partly yields an additional red-shifted ring-open species absorbing at λ_{max} = 734 nm, ascribed to the extendedly conjugated quinoidal open form, which is not observed though direct irradiation with UV light of the bispiro closed form. This synthetic methodology opens up to a new family of responsive materials by simple modification of long-established spiropyran syntheses. Moreover, the different states accessible in these bispiropyrans are remarkably stable, allowing for long lived manipulation of the system and dynamic control over properties. The extra species observed give more insight to the inner workings of spiropyrans, as well as their complex isomerization and access thereof. The robustness of the present system, its high switching rates and, as opposed to spiropyrans, their full thermal control with pH-gating opens up to new opportunities for regulating an unprecedented degree of complexity.

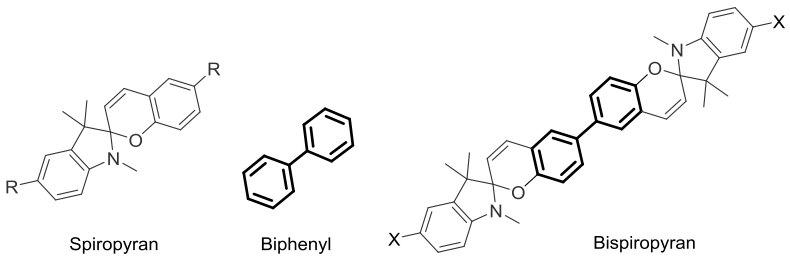

Manuscript in preparation, L. Kortekaas, J. D. Steen, D. Jacquemin, W. R. Browne. Supporting information can be found at the end of the chapter.

Introduction

Molecular switches have been envisioned to play part in reversibly diversifying macroscopic properties by simple stimuli, e.g. irradiation,[1] heat,[2,3] electricity[4] and pH,[5] just as they do on the microscale. The attempted translation from microscopic to macroscopic response commonly involves surface modifications or incorporation into polymers.[6] Many of such incorporable stimuli responsive compounds have been devised to date, photochromic dithienylethenes,[7] stilbenes,[8] and spiropyrans[9] to name but a few that have had a prominent place herein. In search for the ideal behavior a vast range of modifications in these photochromic building blocks have been explored, putting their versatility to the test for decades already. An unpredictable challenge in combining components, however, is cross-compatibility of functionalities, which can have a major impact on the extent of both the retention and the nature of photophysical properties in the final device, sometimes giving rise to new functionality altogether.[10] One way of maximizing this cross-talk in hopes of extending the functionality is to tether the functional groups close together either directly or even by fusing a common motif.[11,12] Wegener *et al.*, for example, show modulation of the antibiotic activity of a drug by UV-triggered switching of an intrinsic stilbene moiety.[13] Areephong *et al.* successfully demonstrated two-part functionality in a terthiophene-diarylethene hybrid, the behavior of which resembled that of the diarylethene in its ring-open form, while changing to that of the terthiophene substituents in the ring-closed form.[11] Conversely, building a spacer unit in between the components has been shown to reduce the change in photophysical properties, confirming a direct relationship between the distance of the functional groups and their electronic communication.[14]

As one of the most synthetically and functionally flexible systems to date, the spiropyran class of photochromes has already shown proficiency at modulating a range of properties in polymers and at surfaces.[9] Their marked influence over properties originates from the strong change in molecular structure upon photochemical breaking of their heterocycle followed by a stabilizing *Z/E* isomerization (**Scheme 1**). While several so called *transoid* merocyanine forms are conformationally possible, the *TTC* form, as by the *cis-trans* configuration about the α, β and γ positions in the pyran alkene bridge, has been shown to be the thermally most stable with a small presence of *TTT* form depending on solvent (see Chapter 1). Moreover, in acetonitrile specifically it has been shown that this ratio of *TTC* to *TTT* isomer of 6-nitrobenzoindolinospiropyran is 10:1, and that the *TTT* form has a red-shifted absorption maximum at 595 nm compared to that of *TTC* at 557 nm.[15]

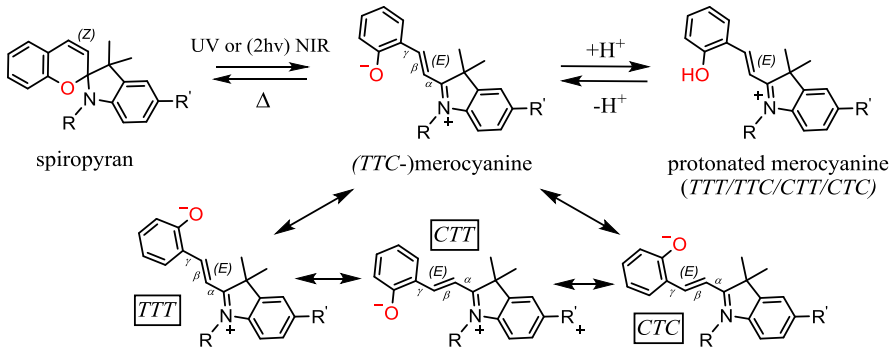

Scheme 1. Photochemical conversion of the ring-closed spiropyran to the ring-open merocyanine form with thermal reversion. The *TTC* ring-open merocyanine form, with *C* and *T* indicating their *cis* and *trans* configuration about the α, β and γ positions, commonly is thermally most stable, but the other *transoid* isomers may be thermally accessible as well. Protonation of the colored merocyanine form obstructs the ring-closing by generating a thermally stable state.

The photoconversion to the zwitterionic ring-open isomers is reversible by heat and, as shown in Chapter 5, can be avoided by conversion to the thermally stable protonated form upon treatment with strong acids. This intrinsic behavior was also already observed in bis-spiropyrans[16] while making use of the ability of spiropyrans to undergo oxidative coupling (Scheme 2).[17]

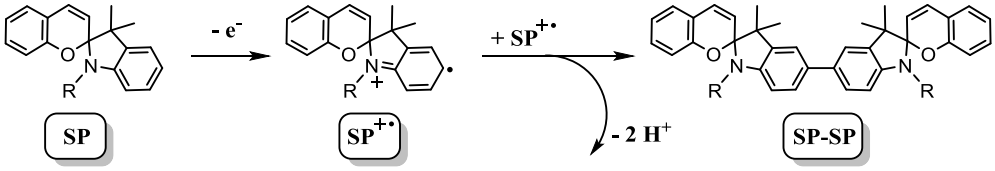

Scheme 2. Oxidative (electrochemical) indoline-indoline coupling of spiropyrans to bis-spiropyran dimers as first described by Ivashenko *et al*.[17]

In this present work we take advantage of the modularity of spiropyrans while building on the previously reported bis-spiropyran system by re-approaching their dimeric tethering. Here, we take on an alternative route by synthetically linking two spiropyrans directly through their pyran unit instead of their indoline fragment, with a biphenyl central motif as a result (Scheme 3). This was achieved by chemical aryl-aryl coupling of 5-iodosalicylaldehyde with a palladium/indium bimetallic system according to literature procedure,[18] followed by double Fischer base condensation of the indoline to the double spiropyran (*vide infra*).

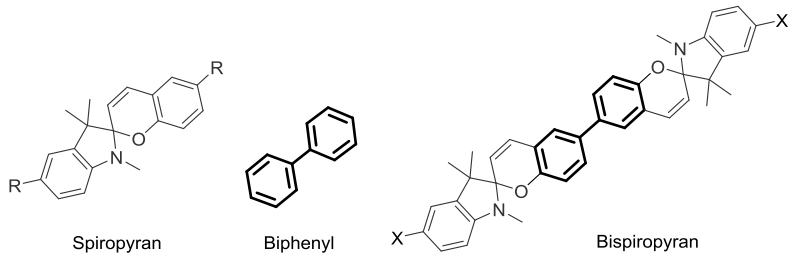

Scheme 3. A new approach towards coupling spiropyran photochromes, direct linking through the pyran unit.

We show that, alike its single spiropyran precursor (see Chapter 5), the bispiropyran (biSP) photoswitch possesses swift thermal reversion from the bimerocyanine (biMC) form and protonates to the deprotonated bimerocyanine ($biMCH_2^{2+}$) spontaneously upon addition of trifluoromethanesulfonic (triflic) acid. Furthermore, though the pH-gated photoisomerization seen in Chapter 5 is retained, an electronic structure additional to the usual *TTC* form is observed upon deprotonation. This structure is ascribed to that of the quinoidal double *TTC* isomer which is stabilized by increased orbital overlap throughout the *trans*-configuration over the full photochrome (Scheme 4), thus ultimately overcoming the energetic stability of the zwitterionic *TTC* form which is stabilized by phenolate H-bonding with the C_3'-H.

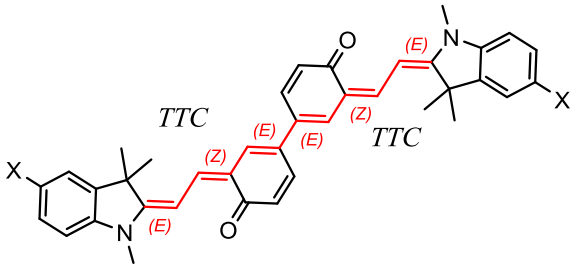

Scheme 4. Structure of the doubly *TTC* quinoidal form of bispiropyran, accessed through the reversible breaking up of the *TTC* stabilizing H-bonding between the phenolate and the C_3'-H.

The novel photochemical activity and stability of their different states that is shown by this species is unprecedented and opens up to new uses for this class of spiropyran based photochromes.

Experimental section

Materials. All of the chemicals for the synthesis of **1**, **2** and **3** were purchased from Aldrich or TCI and were used without further purification. HPLC grade acetonitrile was used without additional purification for the spectroscopic measurements.

Synthesis of 1. 74.0 mg $Pd(PPh_3)_4$ (0.064 mmol, 4 mol %) and 273.5 mg In (2.4 mmol, 1.5 eq.) was added at room temperature to a solution of 5-iodosalicylaldehyde (400.5 mg, 1.6 mmol) in 8 mL DMF and the resulting mixture heated to 100 °C for 72 h. After cooling to room temperature the reaction mixture was quenched with 15 mL of semisaturated $NaHCO_3$. An extraction with EtOAc (3 x 20 mL) was followed by washing of the organic layer with water (2 x 30 mL) and brine (20 mL), with subsequent drying over $MgSO_4$. The organic layer was dried in vacuo and the residue was transferred to a P4 glass filter with washing by pentane and scraping the compound out of the flask (3 x 30 mL). The pentane removed almost all of the residual monomer present, yet a final washing with a small amount of diethyl ether (5 mL) gets rid of the last portion, yielding 77.0 mg of yellow crystals (0.32 mmol, 20% yield). ^{1}H NMR ($CDCl_3$, 400 MHz): δ 11.01 (s, 2 H), 9.99 (s, 2 H), 7.73 (m, 4 H), 7.10 (d, J = 9.76 Hz, 2 H).

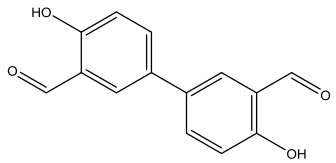

Synthesis of 2. 1,3,3-trimethyl-2-methyleneindoline (76.0 mg, 0.43 mmol) was added to a solution containing 32.2 mg of **1** (0.13 mmol) in 15 mL EtOH followed by refluxing for 20 h under Argon. Pinkish-white crystals had crashed out the solution, which is still highly colored from the excess of 1,3,3-trimethyl-2-methyleneindoline. The reaction mixture was cooled down to 0 °C and filtered over a P4 glass filter, with subsequent washing of the filtrand by a small amount of EtOH at 0 °C, turning the crystals white (30.4 mg, 0.06 mmol, 42% yield). Chloroform is sufficiently acidic of nature to partly ring open the product into various isomers, whereas acetonitrile provides a clean spectrum of solely the ring closed form. ^{1}H NMR (CD_3CN, 400 MHz): δ 7.37 (d, J = 2.22 Hz, 2 H, i), 7.33 (dd, J = 2.36 Hz and J = 8.41 Hz, 2 H, j), 7.15 (dt, J = 0.98 Hz and J = 7.73 Hz, 2 H, b), 7.11 (d, J = 6.71 Hz, 2 H, d), 7.01 (d, J = 10.20 Hz, 2 H, h), 6.82 (t, J = 7.25 Hz, 2 H, c), 6.66 (d, J = 8.44 Hz, 2 H, k), 6.57 (d, J = 7.68 Hz, 2 H, a), 5.81 (d, J = 10.23 Hz, 2 H, g), 2.73 (s, 6 H, l), 1.29 (s, 6 H, e/f), 1.15 (s, 6 H, e/f).

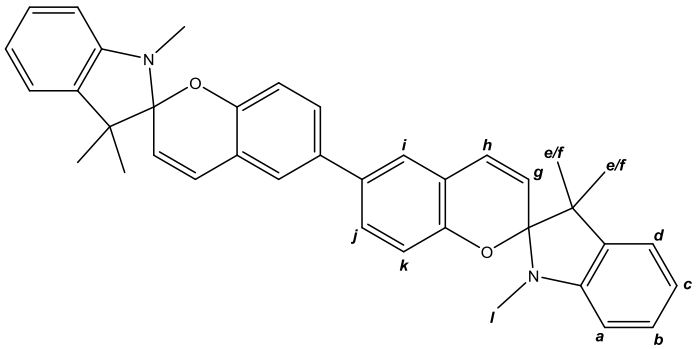

Synthesis of 3. 1,3,3-trimethyl-2-methyleneindoline (172.8 mg, 0.83 mmol) was added to a solution containing 66.5 mg of **1** (0.27 mmol) in 40 mL EtOH followed by refluxing for 20 h under Argon. Pinkish-white crystals had crashed out the solution again, the solution still being highly colored from the excess of 1,3,3-trimethyl-2-methyleneindoline. The reaction mixture was cooled down to 0 °C and filtered over a P4 glass filter, with subsequent washing of the filtrand by a small amount of EtOH at 0 °C, turning the crystals to off-white (41.8 mg, 0.07 mmol, 25% yield). Chloroform is sufficiently acidic of nature to partly ring open this product as well into various isomers, whereas acetonitrile provides a clean spectrum of solely the ring closed form. ^{1}H NMR (CD_3CN, 400 MHz): δ 7.37 (d, J = 2.14 Hz, 2 H, h), 7.33 (dd, J = 2.26 Hz and J = 8.37 Hz, 2 H, i), 7.14 (dd, J = 2.18 Hz and J = 8.07 Hz, 2 H, b), 7.10 (d, J = 2.02 Hz, 2 H, c), 7.01 (d, J = 10.17 Hz, 2 H, g), 6.67 (d, J = 8.37 Hz, 2 H, j), 6.52 (d, J = 8.39 Hz, 2 H, a), 5.79 (d, J = 10.26 Hz, 2 H, f), 2.71 (s, 6 H, k), 1.27 (s, 6 H, d/e), 1.15 (s, 6 H, d/e).

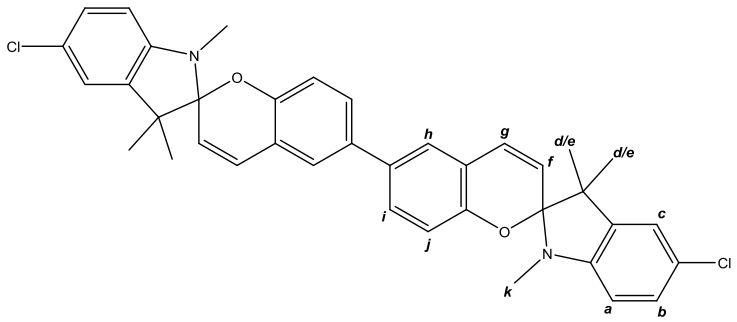

Physical methods. ^{1}H and ^{13}C NMR spectra were obtained on a Bruker 600 spectrometer. Chemical shifts (δ) are reported in parts per million and coupling constants in Hertz. Multiplicities are denoted as follows: s = singlet, d = doublet, t = triplet, br = broad singlet, m = multiplet. Chemical shifts are reported with respect to tetramethylsilane and referenced to residual solvent (CHD_2CN) signals. UV/vis absorption spectra were obtained on an Analytik Jena Specord600 spectrometer. Irradiation at 300 nm (370 µW), 365 nm (4.1 mW), 455 nm (3.2 W), 490 nm (2.3 mW), 565 nm (2.0 mW), and 660 nm (14.5 mW) was provided by M300F2, M365F1, M455L3-C5, M490F1, M565F1 and M660F1 Thorlabs laser diodes. UV/vis absorption spectra recorded at -30 °C used a QuantumNorthwest temperature controlled cuvette holder. Absolute quantum yields were determined as described in Chapter 5. Emission spectra were obtained by excitation with the aforementioned laser diodes, with a 500 nm shortpass filter in front of the M490F1 LED lightsource specifically in the case of the fluorescence of *E*-**biMCH$_2^{2+}$**.

Results and Discussion

Bisalicylaldehyde **1** was synthesized using an aryl-aryl coupling procedure reported by Chang et al.[18] Bispiropyrans **2** and **3** were prepared by Fischer base condensation of 1,3,3-trimethyl-2-methyleneindoline and 5-chloro-1,3,3-trimethyl-2-methyleneindoline, respectively, with the bisalicylaldehyde (**Scheme 5**), and characterized by ^{1}H and two-dimensional NMR spectroscopy.

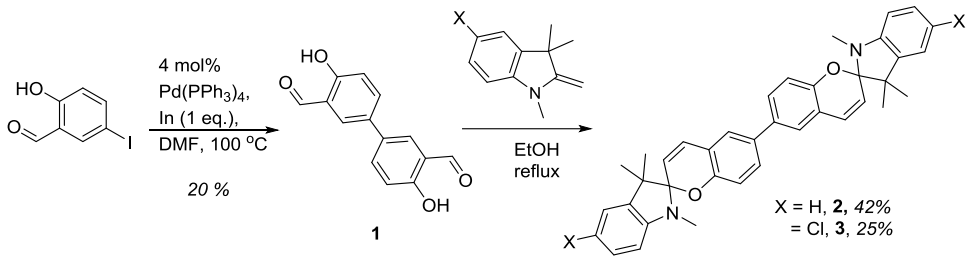

Scheme 5. Synthesis of bispiropyrans **2** and **3**.

Photochromism of bispiropyrans:

Bispiropyrans **2** and **3** show UV-vis absorption spectra that are typical of spiropyrans with absorption only in the UV region, with irradiation at room temperature resulting in only a slight transient increase in visible absorption (**Figure S1**). The absence of photochromic behavior at room temperature is due to rapid thermal reversion as at -30 °C photo induced ring-opening is observed (**Figure S1**) with a quantum yield for **3** of 4 %, which is similar to that of unmodified spiropyrans (ca. 7 %, see chapter 5). Both **2** and **3** show maxima at 395 and 619 nm with a shoulders at 408 and 660 nm, respectively (**Figure 1**, right and **Figure S2**). Subsequent irradiation with visible light did not affect the spectra of the open bimerocyanines (**Figure S1**), as expected for spiropyrans without electron withdrawing substituents (see Chapter 1). In comparison, the monospiropyran shows maximum absorption at 385 nm and 582 nm, with only a shoulder at 398 nm.

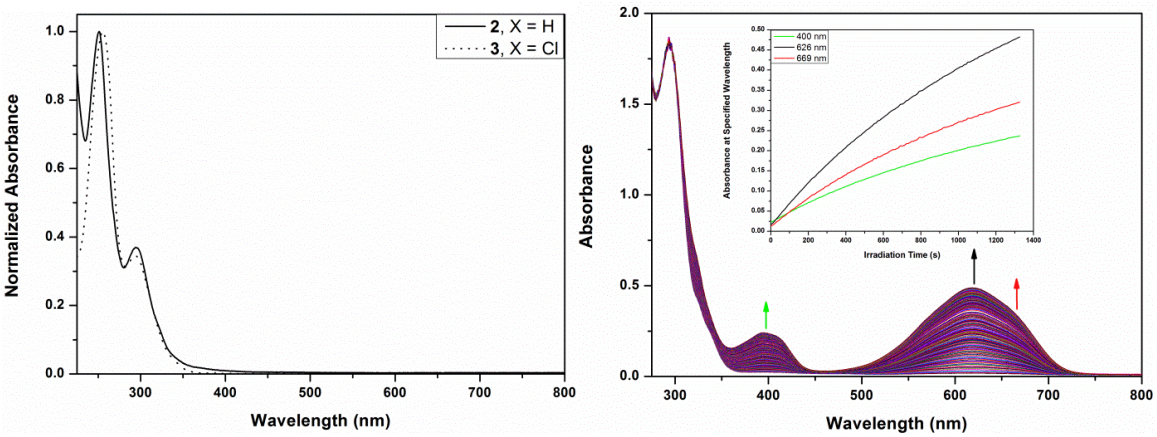

Figure 1. (left) Normalized UV/vis absorption of **2** (solid) and **3** (dashed) in acetonitrile and (right) UV/vis absorption spectroscopy (-30 °C) of **2** in acetonitrile during irradiation at 300 nm.

pH-gating and acidochromism of bispiropyrans:

The pH-gating and acidochromism of spiropyrans discussed in chapter 5 is observed for the bispiropyrans **2** and **3** also. An instant response to addition of stoichiometric triflic acid is observed with spontaneous ring opening to the *Z*-bimerocyanines (**Figure 2**, left). Incremental addition of acid results in a stepwise change in absorbance without evidence for intermediate species even at low temperature. Subsequent deprotonation recovers the absorption spectrum of the ring-closed form immediately (**Figure S3**). Irradiation of the protonated form results in the appearance of absorption bands at 385 and 450 nm (compared to 420 nm for spiropyran, Chapter 5) with an isosbestic point maintained at 350 nm, suggesting *Z*/*E*-isomerization proceeds without

significant steady state concentrations of intermediates (**Figure 2**, right). The quantum yield is 68 %, which is similar to that (92 %) of the monospiropyran (see chapter 5). In contrast to the monospiropyrans, however, thermally induced interconversion of the *Z*- and *E*-isomers is not observed, and irradiation at 455 nm does not induce reversion (*E* to *Z*) in the bispiropyrans. In summary, protonation results in formation of two thermally stable open isomers at room temperature, with one formed from the other by irradiation with UV light (**Scheme 6**, **Figure S4**).

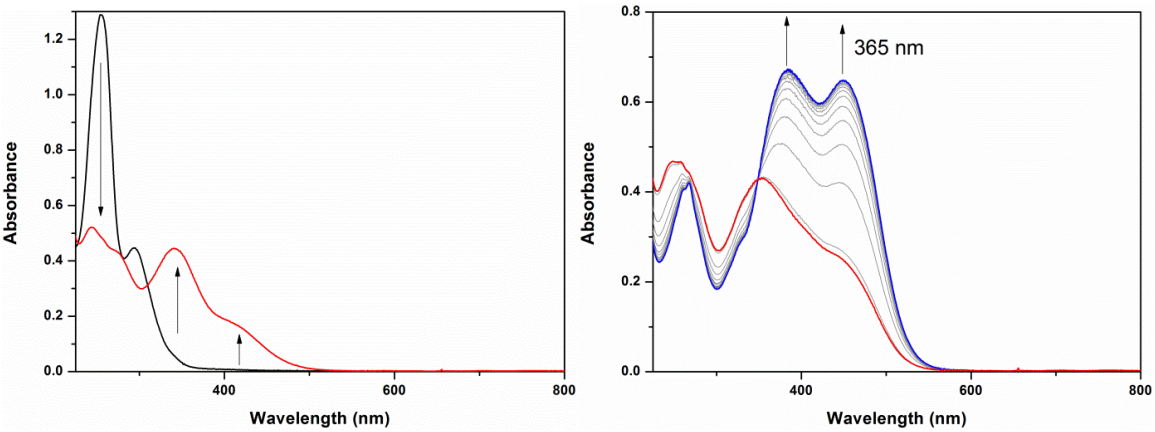

Figure 2. (Left) UV/vis absorption spectrum of **3** (35 µM in acetonitrile) upon addition of 2 equiv. CF_3SO_3H to form the *Z*-biMCH$_2^{2+}$ form and (right) subsequent irradiation at 365 nm to form the *E*-biMCH$_2^{2+}$ form.

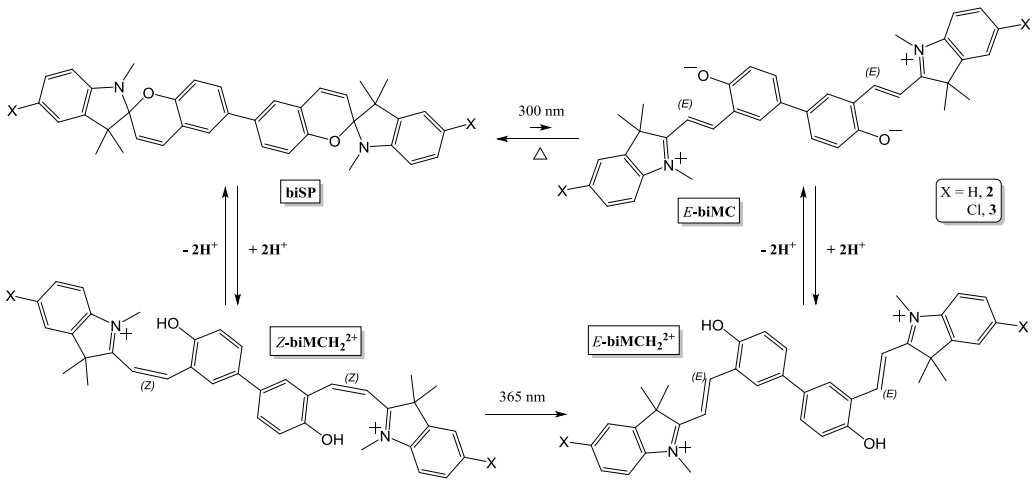

Scheme 6. Dual photo- and pH-switching of **2** and **3** with fast thermal reversion of the unprotonated bimerocyanines, but full thermal stability at room temperature in the protonated states concurrent with unidirectional photoisomerization.

Deprotonation of **2** or **3** with Et_3N or sodium acetate recovers the merocyanine form, which relaxes quickly to the closed spiro form at room temperature. However, in contrast to the monospiropyran additional absorption bands at 310 and 730 nm are observed (**Figure S5**). The additional species is not observed upon irradiation of the spiro form at low temperature, and its absorption undergoes thermal decay more rapidly than that of bimerocyanine.

pH-gating of photo induced extended conjugation in bispiropyrans:

At -30 °C *Z*/*E*-isomerization is observed upon addition of 2 equiv. of CF_3SO_3H to **2** or **3** followed by irradiation at 365 nm (**Figure S6**). Subsequent addition of base in a stepwise manner results in a more pronounced absorption at 730 nm than observed at room temperature (**Figure 3**).

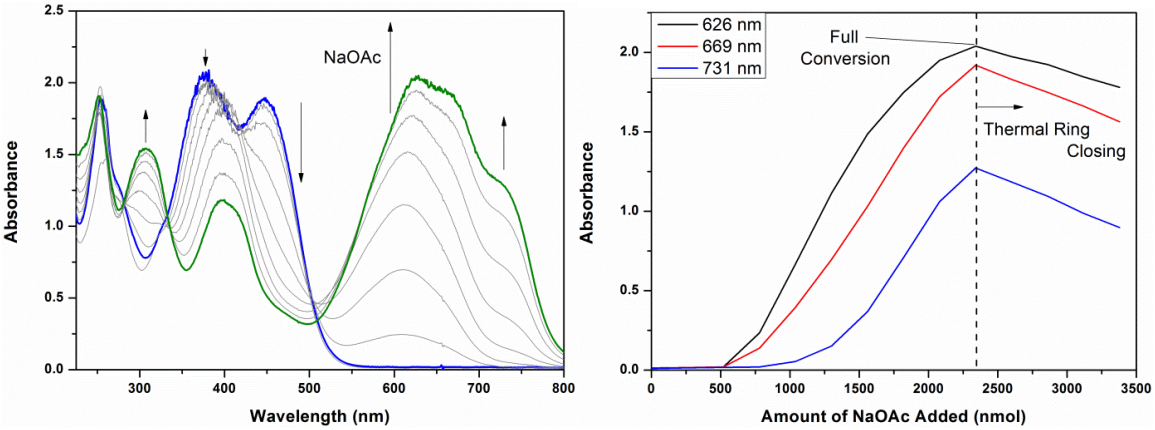

Figure 3. (Left) UV/vis absorption spectrum (at -30 °C) of (blue) *E*-biMCH$_2^{2+}$ in acetonitrile (generated by irradiation of **2** with 2 equiv. CF_3SO_3H present) with subsequent addition of NaOAc (260 nmol per step) and (right) the evolution of absorbance at selected wavelengths as base is added. At 2340 nmol base added full conversion is reached (dotted line), and the subsequent few additions merely showed thermal decay of visible absorption.

After full deprotonation, the thermal decay of the extra species also occurs gradually at -30 °C, and is completely independent of visible light irradiation as well (**Figure S7**). Interestingly, avoiding exposure to UV light during the deprotonation favors the formation of the NIR absorbing species, thereby enabling distinguishing between the bimerocyanine form generated by direct irradiation and the extra species generated by pH switching (**Figure 4**).

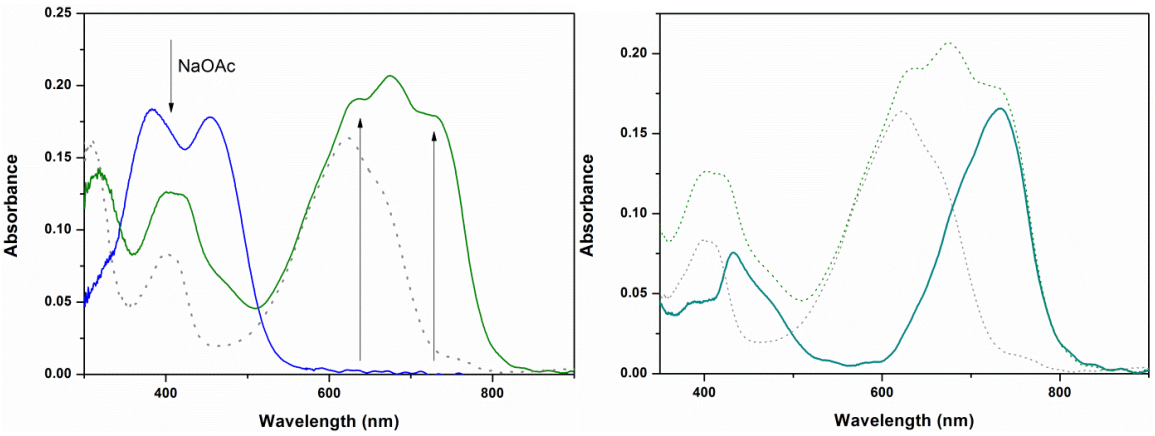

Figure 4. UV/vis absorption spectrum (at -30 °C) of **3** in acetonitrile, before and after excitation with a halogen light source. (Left) After photogeneration of *E*-biMCH$_2^{2+}$ (blue line) an excess 1200 nmol NaOAc was added, creating a mix of the previously observed *E*-bimerocyanine absorption (normalized trace added as dotted grey line) and the new NIR species. (Right) Absorption spectrum of the new species with λ_{max} at 734 nm obtained by scaled subtraction of the spectrum of *E*-merocyanine (grey dotted line) from the spectrum of a mixture of both species (green dotted line).

^{1}H NMR spectroscopy of bispiropyrans:

As with spiropyrans, the stability of the accessible bispiropyran/bimerocyanine forms allows for their observation by ^{1}H NMR spectroscopy. Unlike with spiropyrans, which are unable to fully convert to the *E*-isomer due to a photostationary state, a complete series of thermally stable bispiropyran states can be characterized in order by ^{1}H NMR spectroscopy at room temperature (**Figure 5, Table 1**).

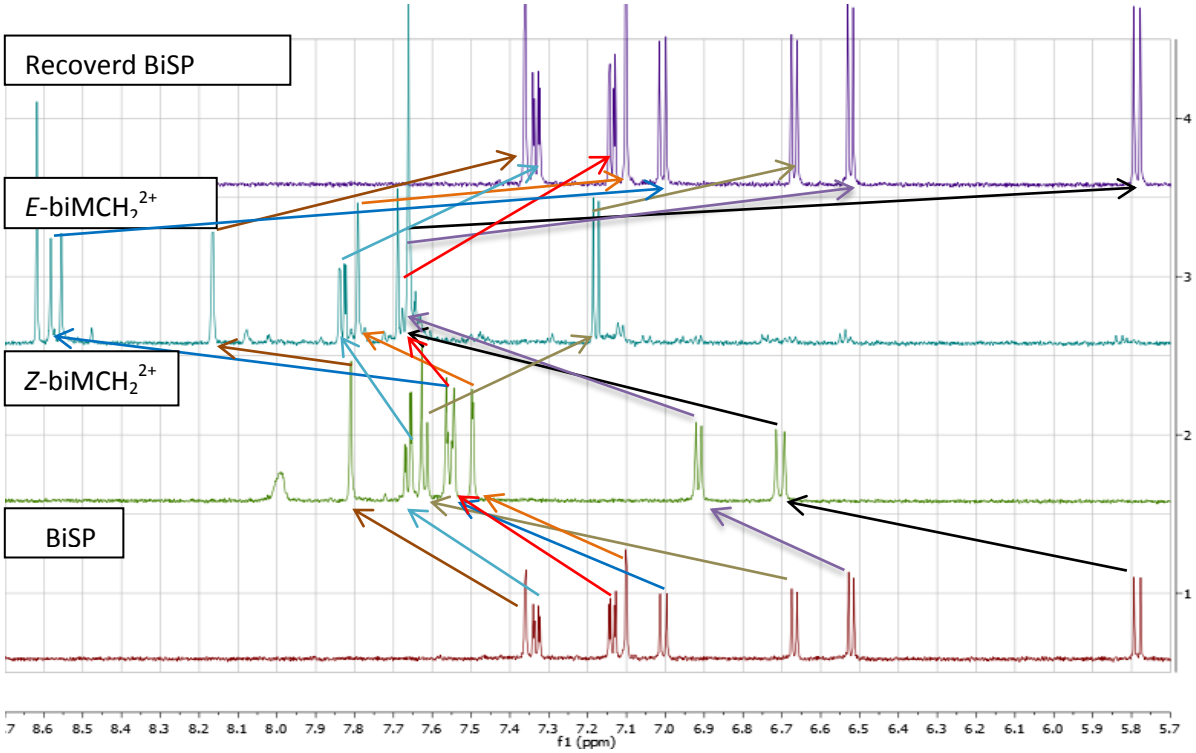

Figure 5. ^{1}H NMR spectra of bispiropyran **3** (1, bottom), with 2 equivalents of CF_3SO_3H (2), after subsequent irradiation at 365 nm (3), and upon addition of 21 equivalents of sodium acetate (4).

	BiSP		*Z-biMCH$_2^{2+}$*		*E-biMCH$_2^{2+}$*	
Proton	*Chemical Shift*	*Coupling*	*Chemical Shift*	*Coupling*	*Chemical Shift*	*Coupling*
l	-	-	7.99 (bs)	-	-	
h	7.36 (d)	2.28	7.81 (d)	2.01	8.18 (d)	2.31
i	7.33 (dd)	8.36/2.36	7.66 (dd)	8.52/1.97	7.84 (dd)	8.54/2.32
b	7.14 (dd)	8.19/2.20	7.55 (m)		7.65 (m)	-
c	7.10 (d)	2.10	7.50 (d)	2.40	7.79 (d)	1.59
g	7.00 (d)	10.20	6.71 (d)	12.93	7.68 (d)	16.41
j	6.67 (d)	8.30	7.62 (d)	8.59	7.20 (d)	8.53
a	6.52 (d)	8.20	6.92 (d)	8.41	7.65 (m)	-
f	5.78 (d)	10.17	7.55 (m)		8.57 (d)	16.40
k	2.71 (s)	-	3.32 (s)	-	4.00 (s)	-
e	1.27 (s)	-	1.65 (s)	-	1.81 (s)	-
d	1.15 (s)	-	1.65 (s)	-	1.81 (s)	-

Table 1. ^{1}H NMR chemical shift assignments of **3** in its different states, chemical shift (δ) in ppm, multiplicity in parentheses, coupling constant in Hz.

In comparison, spiropyran, which has been shown to undergo spontaneous conversion to the *Z*-merocyanine upon protonation followed by *Z*/*E*-isomerization under UV irradiation, shows almost identical chemical shifts and coupling constants (see Chapter 5). The ^{1}H signal of the methane closest to the indoline (proton **f**) shifts from 5.75 ppm to 7.64, and further to 8.52 ppm upon *Z*/*E*-isomerization, with coupling constants changing from 10.25 Hz via an unidentifiable multiplet to 16.43 Hz in the *E* isomer. Concomitantly the signal of the hydrogen on the side of the phenol (proton **g**) shifts from 6.94 ppm to 6.66, and further to 7.57, with the coupling constants changing from 10.25 Hz via 12.82 Hz in the *Z*-isomer to 16.43 Hz in the *E* isomer as well.

Although it is not observed by UV/vis spectroscopy (**Figure S3**), stepwise addition of triflic acid allows for an intermediate species to be observed by ^{1}H NMR spectroscopy (**Figure 6**). This intermediate indicates that instead of the first protonation rendering the second protonation step more facile, a thermally stable intermediate is formed, possibly a form of the singly protonated species (**Scheme 7**), while the electronic structure still resembles that of the ring closed form. The coupling constant of the intermediate's signals at 5.80 ppm (chemical shift of +0.01 ppm with respect to the closed spiro form) and 6.94 ppm (a shift of -0.07 ppm) are 10.05 Hz, while the aliphatic methyl protons undergo shifts of 0.01 ppm.

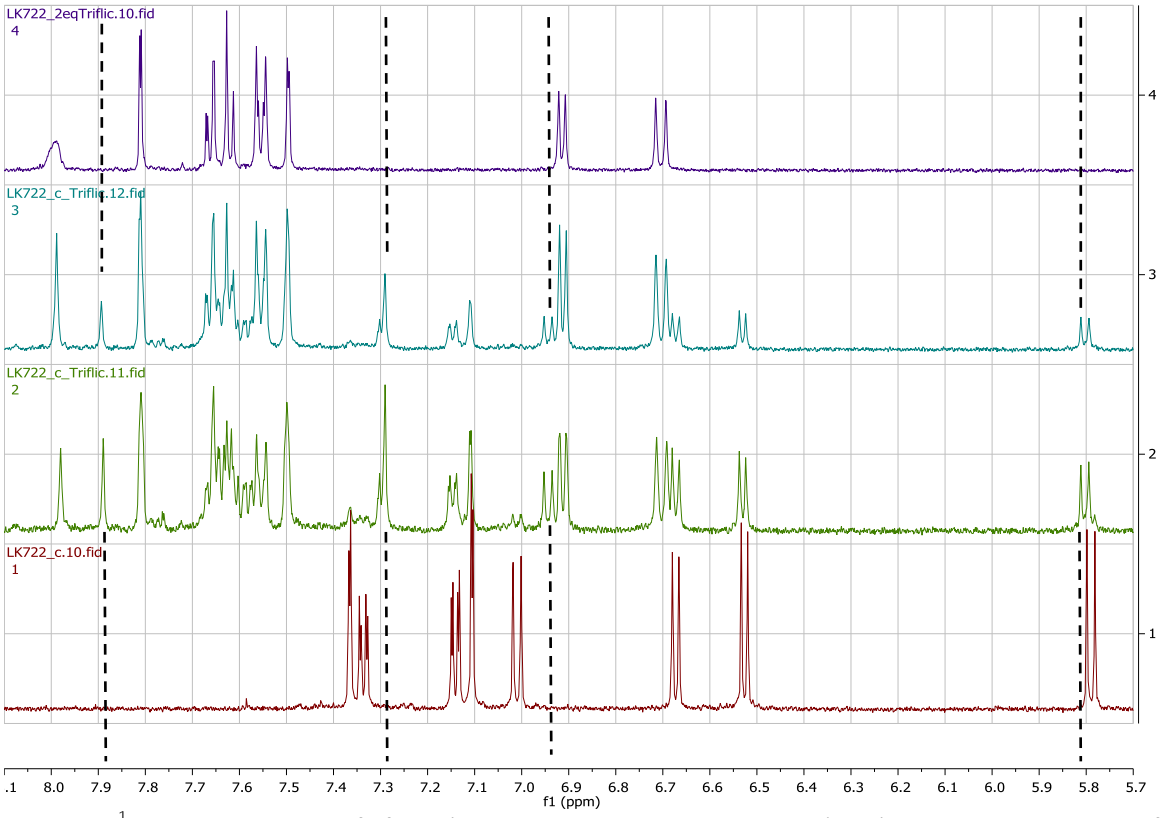

Figure 6. ^{1}H NMR spectrum of, from bottom to top, **3** in CD_3CN, and with increasing amounts of trifluoromethanesulfonic acid to the complete conversion to protonated bimerocyanine form.

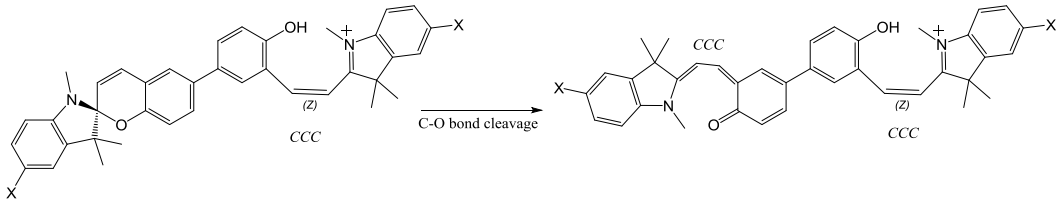

Scheme 7. Possible intermediate protonation state of bispiropyrans.

^{1}H NMR spectroscopy at -30 °C with in situ irradiation:

As for UV/vis absorption spectroscopy at low temperature, the increased lifetime of intermediate species formed upon protonation and irradiation allows for their study by ^{1}H NMR spectroscopy. Irradiation of the protonated bimerocyanine at 365 nm at -30 °C results in the appearance of several species before conversion to the final photoproduct (**Figure 7**).

Figure 7. Evolution of ^{1}H NMR spectrum of **2** in acetonitrile-d_3 after protonation during *in situ* irradiation (λ_{exc} = 365 nm, spectra arranged from bottom to top).

Minor shifts in the ^{1}H signals of the alkene and aliphatic methyl substituents indicate that a conformational change occurs during irradiation at 365 nm. Eventually the most thermodynamically stable state is reached, presumed to be the *TTC* form.

Fluorescence spectroscopy of bispiropyrans:

Emission of **3** was studied at -30 °C to investigate fluorescence properties of the different states of bispiropyrans. Interestingly, apart from the closed form (λ_{exc} = 300 nm) neither the *Z*-**biMCH$_2^{2+}$** (λ_{exc} = 365 nm and 420 nm) nor the unprotonated ring-open *E*-**biMC** (λ_{exc} = 565 nm, 660 nm and 691 nm) emitted upon irradiation. The protonated *E*-**biMCH$_2^{2+}$** form, however, emits red light when irradiated at λ_{exc} = 490 nm (**Figure 8**). This provides a single, but thermally completely stable emissive state, reached by protonation and irradiation with UV light and reverted by facile addition of base.

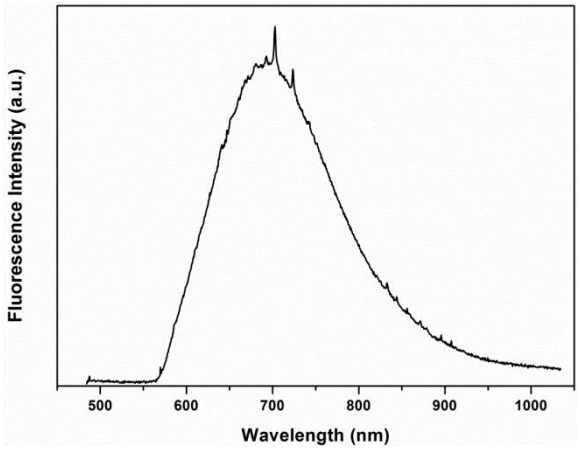

Figure 8. Emission spectrum of **3** in acetonitrile at -30 °C (λ_{exc} = 490 nm).

Conclusions

Here, we have shown that when tethering two spiropyrans together through their pyran component the photochromism to the ring open bimerocyanine at low temperature is retained, as well as the pH-gated access to the protonated ring-open forms at room temperature. However, unlike in spiropyrans, the pH-gating leads to two completely thermally stable states, the protonated *E* form being irreversibly photogenerated by irradiation with UV light of the protonated *Z*-bimerocyanine. Once accessed, the *E*-isomer is shown to be a capable red-emitter (λ_{exc} = 490 nm) and at any time the system can be reset by deprotonation, allowing the swift thermal reversion to recover the bispiropyran ring-closed starting form. Furthermore, this deprotonation pathway yields stability in a new isomer which is not observed upon direct irradiation to the ring-open *TTC* form, with a red-shifted absorption maximum at 734 nm. This new isomer is postulated to be the doubly quinoidal *TTC* form which possesses *E*-conjugation over a total of 6 double bonds, supporting the further red-shift that is observed. Overall, this approach of tethering spiropyrans through their photochrome has shown to enhance the thermal stability of the pH-gated photochromism, ultimately providing access to a thermally stable and emissive protonated *E*-form. Additionally, the detection of the intermediate bimerocyanine form which can only be accessed through deprotonation of this *E*-isomer provides further insight into the spectroscopic properties and the behavior of bispiropyrans. This synthetic design thus opens up to a new family of responsive materials by simple modification of long-established spiropyran

syntheses. Moreover, the achieved greatly enhanced thermal stability in these bispiropyrans bring us a step closer to the envisioned long lived manipulation of system dynamics by the spiropyran photochrome. The robustness of the present system and its high switching rate to the structurally different *E* form over mere seconds opens up to new opportunities for providing full control over an unprecedented degree of complexity.

Supporting information

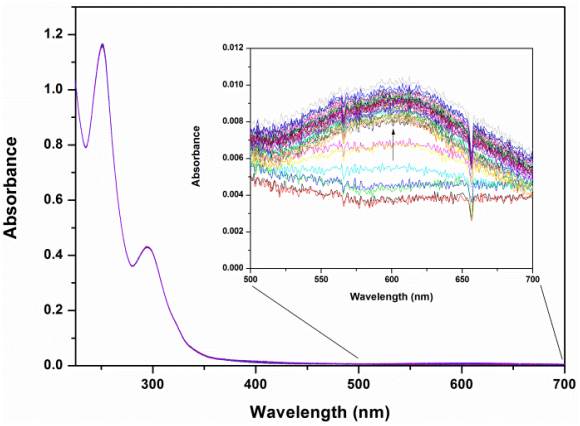

Figure S1. UV/vis absorption spectrum of **2** in acetonitrile over time (arrow) while irradiating at 300 nm.

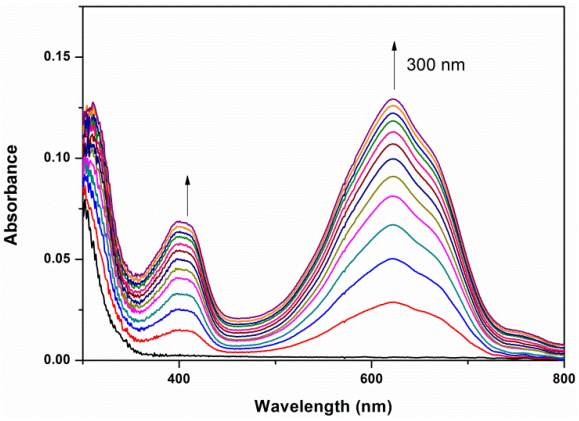

Figure S2. UV/vis absorption spectroscopy (at -30 °C) of **3** in acetonitrile during irradiation at 300 nm.

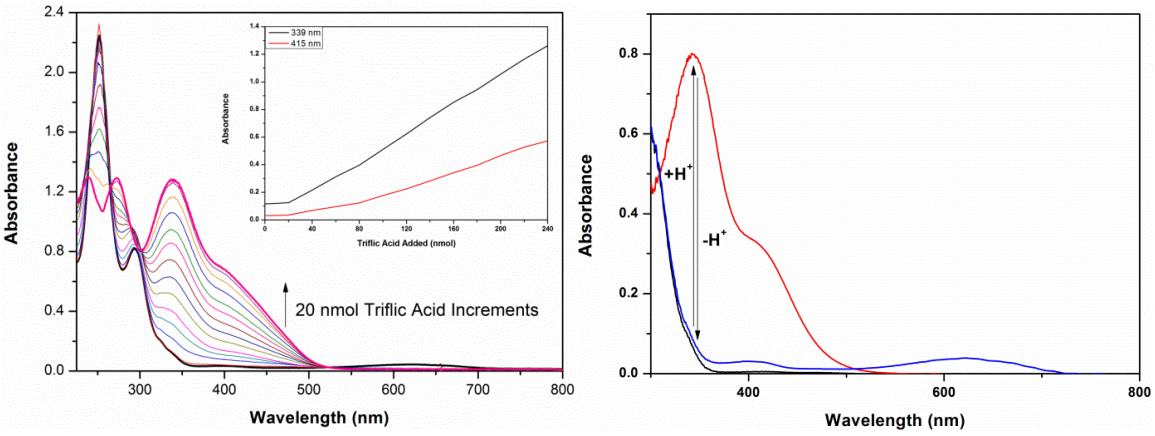

Figure S3. (Left) UV/vis absorption spectroscopy (at -30 °C) of **2** in acetonitrile following addition of triflic acid and (right) addition of 2 equiv. CF_3SO_3H to **3** in acetonitrile, followed by addition of 10 equiv. sodium acetate (note that absorption of merocyanine is observed due to irradiation from the spectrometer light source).

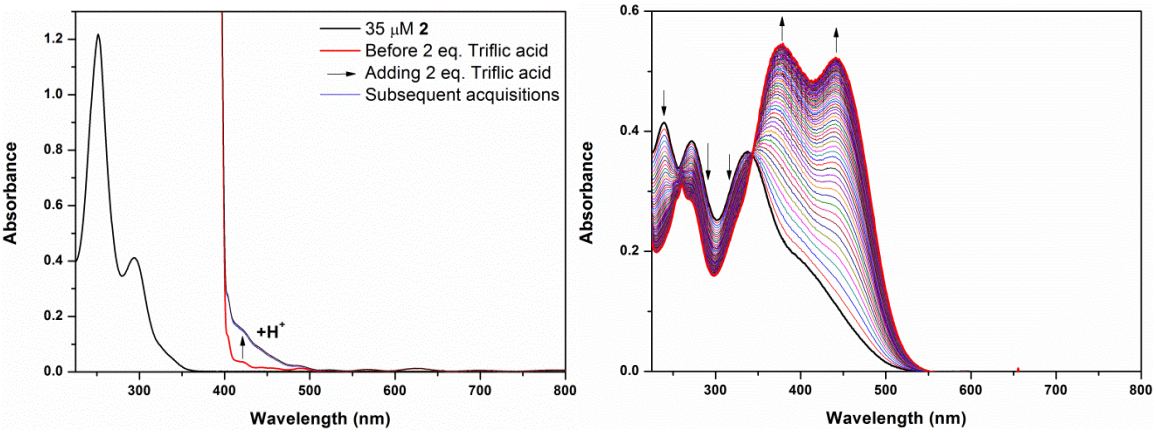

Figure S4. (Left) UV/vis absorption spectra of **2** before (black) and after (red) placing of a 400 nm longpass filter between light source and sample and after addition of 2 equiv. CF_3SO_3H (blue); the spectra is not affected further by 30 spectral acquisitions at 10 s intervals afterward. (Right) UV/Vis absorption spectrum of **2** with 2 equiv. CF_3SO_3H before (black) and under continuous irradiation by the spectrometer. Spectra were recorded at 1 min intervals.

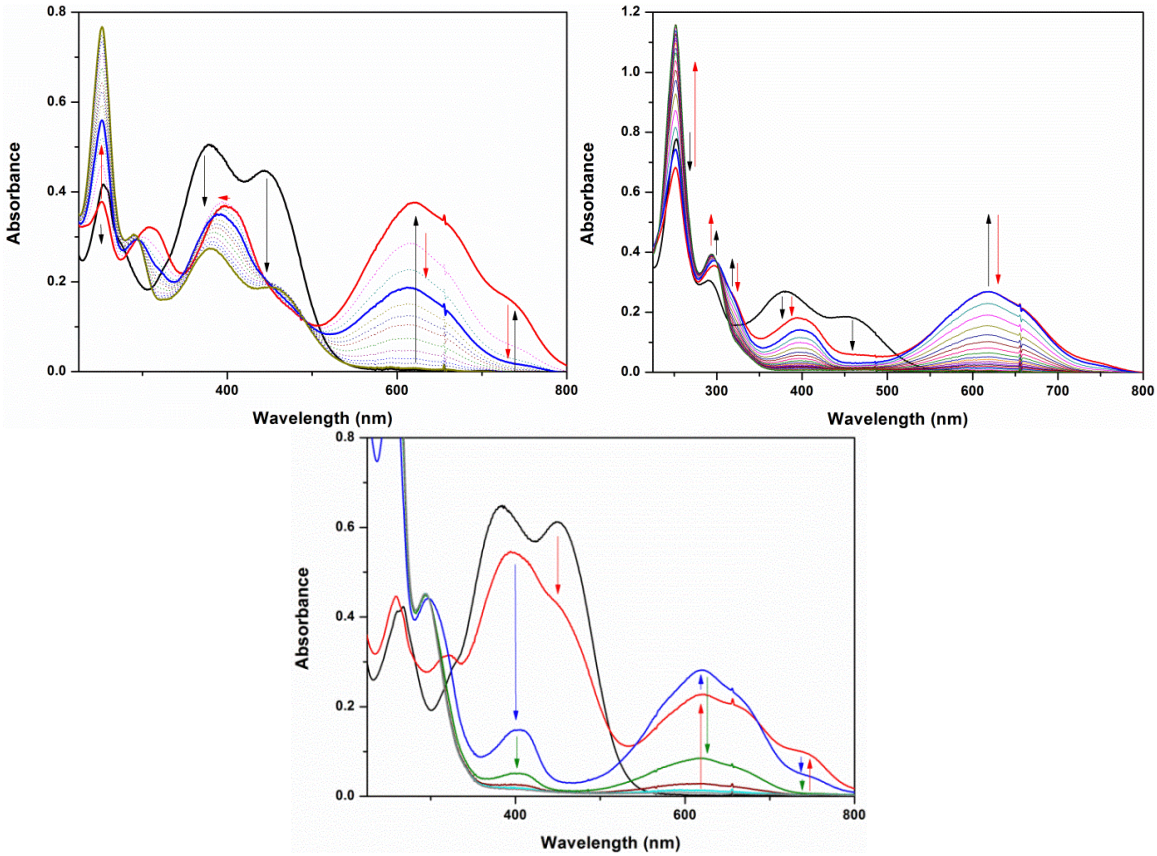

Figure S5. (Top left) UV/vis absorption of **2** in acetonitrile with 2 equiv. CF_3SO_3H after irradiation at 365 nm (black line). Upon addition of 2.5 equivalents of sodium acetate in 50 μL 10:1 acetonitrile/water a new absorption appears rapidly (red line), decaying over time (to blue line) with subsequent full relaxation of the unprotonated bimerocyanine to the closed form. (Top right) Addition of 0.5 more equivalents CF_3SO_3H to deprotonate the remainder of the protonated open form. (Bottom) UV/vis absorption of 35 μM **3** and 2 equivalents of CF_3SO_3H in acetonitrile after irradiating to the photospecies with λ_{exc} = 365 nm, monitored while deprotonating with excess Et_3N. The colored arrows indicate the directions of change in absorption going to the spectrum of their color.

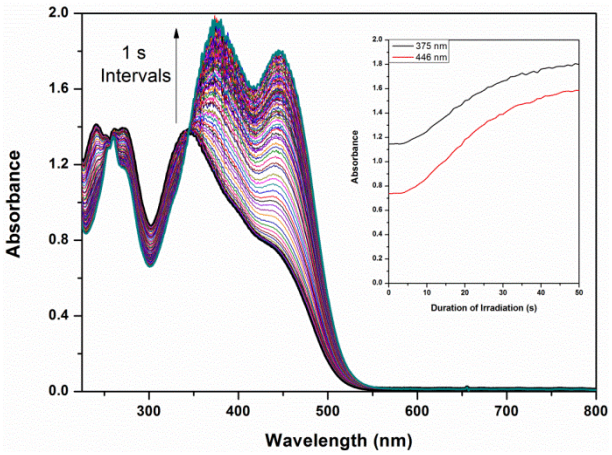

Figure S6. UV/vis absorption spectroscopy (at -30 °C) of **2** in acetonitrile after addition of 2 equiv. CF_3SO_3H (black solid line) upon irradiation at 365 nm.

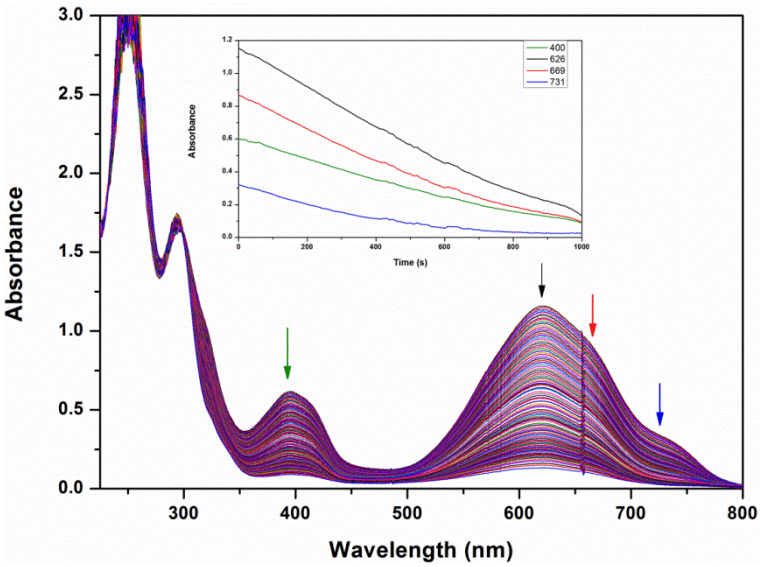

Figure S7. UV/Vis absorption spectrum of bimerocyanine **2** over time in acetonitrile at -30 °C after deprotonating the unknown protonated photospecies. No photoacceleration of this process is observed as the rate of decay does not change by intermediate irradiation at 565 and 660 nm.

References

1 M. Karimi, P. Sahandi Zangabad, S. Baghaee-Ravari, M. Ghazadeh, H. Mirshekari and M. R. Hamblin, *J. Am. Chem. Soc.*, 2017, **139**, 4584–4610.

2 Y. Zhang, Y. Li and W. Liu, *Adv. Funct. Mater.*, 2015, **25**, 471–480.

3 B. Q. Y. Chan, S. S. Liow and X. J. Loh, *RSC Adv.*, 2016, **6**, 34946–34954.

4 Y. Luo and X. Yu, *Eur. Polym. J.*, 2016, **82**, 290–299.

5 Y. Hu, C. H. Lu, W. Guo, M. A. Aleman-Garcia, J. Ren and I. Willner, *Adv. Funct. Mater.*, 2015, **25**, 6867–6874.

6 M. L. Bossi and P. F. Aramendía, *J. Photochem. Photobiol. C Photochem. Rev.*, 2011, **12**, 154–166.

7 M. Irie, T. Fukaminato, K. Matsuda and S. Kobatake, *Chem. Rev.*, 2014, **114**, 12174–12277.

8 R. J. Mart and R. K. Allemann, *Chem. Commun.*, 2016, **52**, 12262–12277.

9 R. Klajn, *Chem. Soc. Rev.*, 2014, **43**, 148–184.

10 L. Kortekaas, F. Lancia, J. D. Steen and W. R. Browne, *J. Phys. Chem. C*, 2017, **121**, 14688–14702.

11 J. Areephong, T. Kudernac, J. J. D. De Jong, G. T. Carroll, D. Pantorott, J. Hjelm, W. R. Browne and B. L. Feringa, *J. Am. Chem. Soc.*, 2008, **130**, 12850–12851.

12 J. Areephong, J. H. Hurenkamp, M. T. W. Milder, A. Meetsma, J. L. Herek, W. R. Browne and B. L. Feringa, 2009, 1–4.

13 M. Wegener, M. J. Hansen, A. J. M. Driessen, W. Szymanski and B. L. Feringa, *J. Am. Chem. Soc.*, 2017, jacs.7b09281.

14 P. Wesenhagen, J. Areephong, T. F. Landaluce, N. Heureux, N. Katsonis, J. Hjelm, P. Rudolf, W. R. Browne and B. L. Feringa, *Langmuir*, 2008, **24**, 6334–6342.

15 S. Ruetzel, M. Diekmann, P. Nuernberger, C. Walter, B. Engels and T. Brixner, *J. Chem. Phys.*, 2014, **140**, 224310.

16 L. Kortekaas, O. Ivashenko, J. T. Van Herpt and W. R. Browne, *J. Am. Chem. Soc.*, 2016, **138**, 1301–1312.

17 O. Ivashenko, J. T. van Herpt, P. Rudolf, B. L. Feringa and W. R. Browne, *Chem. Commun.*, 2013, **49**, 6737–9.

18 Y. M. Chang, S. H. Lee, M. Y. Cho, B. W. Yoo, H. J. Rhee, S. H. Lee and C. M. Yoon, *Synth. Commun.*, 2005, **35**, 1851–1857.